

# Resonant interaction of solitons with extended defects

K. T. STOYCHEV\*, M. T. PRIMATAROWA, R. S. KAMBUROVA

*Institute of Solid State Physics, Bulgarian Academy of Sciences, 1784 Sofia, Bulgaria*

The interaction of nonlinear Schrödinger solitons with extended defects with modified linear, nonlinear and dispersion coefficients is investigated numerically. Repulsive potentials lead to transmission or reflection of the incoming soliton, similarly to the classical-particle case. Attractive potentials yield non-classical behaviour, associated with the wavelike character of the solitons and for a given range of parameters the scattering patterns exhibit periodically repeating regions of trapping and transmission as a function of the length of the defect segment. It is shown that the escape of the soliton is due to a resonance between the period of the shape oscillations of the soliton inside the segment and the length of the latter. Scattering from inhomogeneities involving two modified coefficients is also investigated and peculiarities associated with the complex potential profiles at the boundary are obtained.

(Received November 1, 2006; accepted December 21, 2006)

*Keywords:* Nonlinear Schrödinger equation, Solitons, Inhomogeneities

## 1. Introduction

Nonlinear soliton pulses have been widely investigated due to their stability and information potential. Their interaction with defect and inhomogeneities is of considerable practical importance. The scattering patterns exhibit a variety of outcomes, including resonant and fractal structures [1-5]. Interaction of solitons with extended defects has been studied in [6-10]. In the present work we investigate in detail the interaction of solitons with wide (compared to the soliton length) inhomogeneities in the linear, nonlinear and dispersion terms in the nonlinear Schrödinger (NLS) equation. For attractive potentials and a given range of parameters, we obtain periodically repeating regions of trapping and transmission as a function of the width of the potential. The observed effects are due to the excitation and a following resonant de-excitation of amplitude (shape) oscillations of the soliton at the boundaries of the well.

## 2. Model

The numerical simulations are based on the perturbed nonlinear Schrödinger equation:

$$i \frac{\partial \alpha}{\partial t} + [1 + \mu(x)] \frac{\partial^2 \alpha}{\partial x^2} + 2[1 + \eta(x)] |\alpha|^2 \alpha + \varepsilon(x) \alpha = 0$$

$$\begin{aligned} \mu(x) &= \mu, \quad \eta(x) = \eta, \quad \varepsilon(x) = \varepsilon \quad \text{for } x_1 \leq x \leq x_2 \\ \mu(x) &= \eta(x) = \varepsilon(x) = 0 \quad \text{otherwise} \end{aligned} \quad (1)$$

where  $\alpha$  is the complex amplitude of the nonlinear wave, and  $\varepsilon, \mu, \eta$  describe an inhomogeneity in the linear, dispersion and nonlinear terms, respectively, of length  $N = x_2 - x_1$ .

For a homogeneous medium with  $\varepsilon = \mu = \eta = const$ , Eq. (1) possesses a fundamental bright soliton solution

$$\alpha(x, t) = \varphi_0 \operatorname{sech} \frac{x - vt}{L} e^{i(kx - \omega t)}$$

$$\varphi_0^2 = \frac{1 + \mu}{(1 + \eta)L^2}, \quad k = \frac{v}{2(1 + \mu)}, \quad \omega = k^2 - \varepsilon - \frac{1 + \mu}{L^2} \quad (2)$$

where  $L$  and  $v$  are the width and the velocity of the soliton. For long defect segments ( $N \gg L$ ) the norm

$$P = \frac{2(1 + \mu)}{(1 + \eta)L} \quad (3)$$

and the energy

$$E = \left( \frac{v^2}{4(1 + \mu)} - \frac{1 + \mu}{3L^2} - \varepsilon \right) P \quad (4)$$

in the ideal ( $\varepsilon = \mu = \eta = 0$ ) and the defect ( $\varepsilon = \mu = \eta = const$ ) regions are nearly conserved. This yields the following relations between the parameters  $v_0, L_0$  and  $v, L$ :

$$L = L_0(1 + \mu)/(1 + \eta) \quad (5)$$

$$v^2 = (v_0^2 + 4\varepsilon)(1 + \mu) + 4(\eta^2 + 2\eta - \mu)/3L_0^2. \quad (6)$$

## 3. Numerical results

In the numerical simulations we used a grid of 2000 points in  $x$  and periodic boundary conditions. The effects studied below correspond to the case of wide and slow solitons ( $2L_0 \gg 1, v_0 \ll 1$ ) which preserves the integrity of the soliton during the scattering and eliminates discreteness effects. For a rectangular potential well with  $\varepsilon = 0.007$  and solitons with  $2L = 11.5$  we obtain trapping for initial velocities  $v_0 < 0.04$  and transmission for  $v_0 > 0.06$  for segments with arbitrary length  $N$ . For intermediate

velocities, the scattering pattern as a function of  $N$  exhibits periodically repeating regions of transmission and capture, and occasionally, narrow reflection windows (Fig. 1).

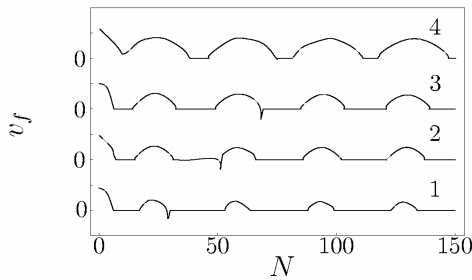


Fig. 1. Final soliton velocity  $v_f$  as a function of the length  $N$  of a defect segment with  $\varepsilon = 0.007$  for different initial velocities  $v_0$ . Curves 1-4 are for  $v_0 = 0.0440, 0.0476, 0.050, 0.0580$ , respectively.

The horizontal parts with zero final velocity correspond to the trapping regions. The regions with positive final velocity correspond to transmission, while the narrow downward spikes with negative final velocity on curves 1-3 correspond to reflection. The relative widths of the regions of transmission and capture depend on the initial velocity and can be quite different, but the period of repeat for  $N > 20$  is nearly constant and depends weakly on the initial velocity.

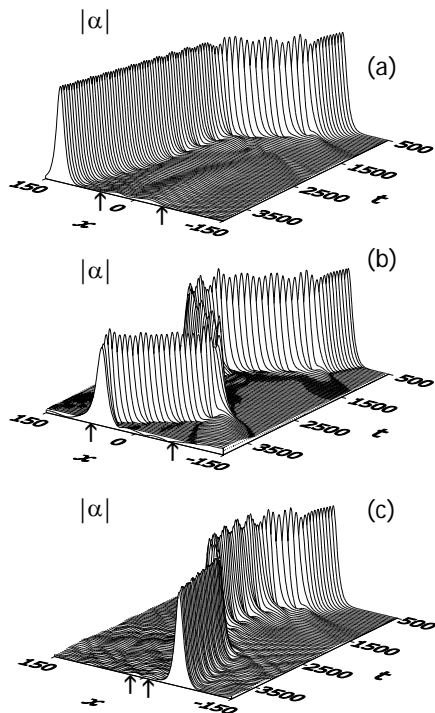


Fig. 2. Evolutionary patterns corresponding to (a) transmission ( $N = 95$ ), (b) trapping ( $N = 110$ ), (c) reflection ( $N=33$ ) for  $v_0 = 0.05$  and  $\varepsilon = 0.007$ . The arrows on the  $x$ -axes mark the boundaries of the segment.

Fig. 2 illustrates the evolutionary patterns corresponding to transmission, trapping and reflection respectively. It is clearly seen that amplitude (shape) oscillations are excited when the soliton enters the potential well and persist while the soliton is inside. Whenever the soliton leaves the defect region, the shape oscillations are strongly suppressed. This suggested that the shape oscillations are the cause of the periodic patterns observed in Fig. 1 and we looked for a correlation between the period of the oscillations and the width of the potential well.

The scattering patterns shown in Fig. 1 have a period of 35 (curve 1) to 36 (curve 4). The temporal period of the shape oscillations evaluated from the data in Fig. 2 is  $T = 208$  and coincides with the soliton period. Shape oscillations of perturbed NLS solitons with the soliton period have been obtained previously in [11-13]. The velocity of the soliton  $v$  inside the segment determined from (6) for initial velocities corresponding to Fig. 1 are in the range 0.173-0.177. The spatial period of the corresponding oscillations thus obtained is  $vT = 36.0-36.8$ , in excellent agreement with the capture-transmission period in Fig. 1. This shows unambiguously that the periodic patterns are due to a resonance between the spatial period of the shape oscillations of the soliton and the length of the segment. The broken periodicity for narrow potential wells ( $N < 20$ ) is due to the smaller interaction energy in this case.

The qualitative explanation of the periodic patterns in Fig. 1 is the following: the inelastic interaction with the first boundary transforms part of the soliton translational energy into weakly decaying shape oscillations. At the second boundary, different outcomes are possible depending on the phase. In the non-resonant case, the reduced energy of the soliton does not allow it to overcome the potential barrier of the second boundary; it is reflected from it and eventually gets trapped. Whenever the time for which the soliton crosses the potential well is commensurate with the period of the shape oscillations (resonance), the inelastic interaction with the second boundary may extinguish the shape oscillations, restoring the soliton energy and allowing it to overcome the barrier and escape. The higher the initial velocity of the soliton the wider the escape regions. In some rare cases the resonant condition for escape is achieved after the soliton has crossed the defect region twice, in the forward and backward directions. This yields the observed narrow reflection spikes in Fig. 1.

We investigated next the interaction of an incoming soliton with a segment with a modified nonlinear coefficient. A segment with a reduced nonlinearity acts as a potential hump and yields transmission or reflection (from the first boundary). A segment with an increased nonlinear coefficient ( $\eta > 0$ ) acts as a potential well and for  $\eta = 0.2$  and initial velocities in the region  $0.038 < v_0 < 0.060$ , the scattering pattern exhibits periodically repeating regions of transmission and capture similarly to the case of a linear-defect segment. The special period is now 20. As can be expected, a smaller nonlinear coefficient (Fig. 3) yields wider transmission

regions and narrower trapping regions and vice versa, while the total period is nearly unchanged.

We investigated also the interaction of NLS solitons with segments with modified group-velocity dispersion coefficient. For “slow” solitons the dependence of  $v$  on  $\mu$  is governed by the last term in (6). Thus, negative values of  $\mu$  lead to an increased velocity inside the segment (potential well), while positive values lead to a decrease of the velocity and act as a potential barrier.

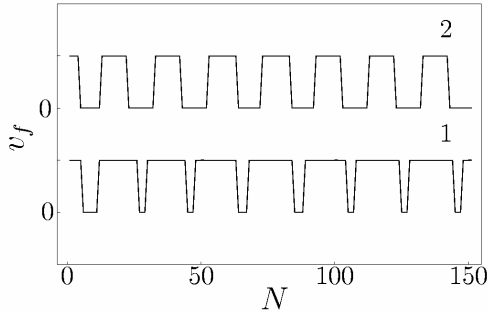


Fig. 3. Periodic regions of trapping and transmission for  $v_0 = 0.05$  and different  $\eta$ . Curve 1:  $\eta = 0.18$ ; curve 2:  $\eta = 0.20$ .

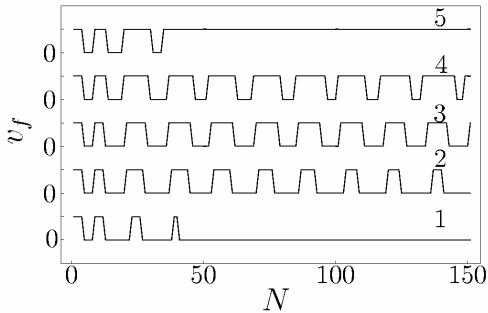


Fig. 4. Regions of capture and transmission for  $\mu = -0.3525$  and different  $v_0$ . Curves 1-5 correspond to  $v_0 = 0.0486, 0.0496, 0.0500, 0.0504, 0.0510$ , respectively.

Fig. 4 shows the scattering results for an attractive potential ( $\mu = -0.3525$ ) and different values of the initial velocity. The capture-transmission patterns in curves 2-4 follow a spatial period of 17. The increase of the initial velocity leads to a wider region of transmission and a narrower region of capture, while the total period remains nearly constant. The broken periodicity in curves 1 and 5 for  $N > 50$  is due to the decay of the shape oscillations into radiation. Thus for very wide segments, the soliton is either transmitted or trapped, depending on whether its final kinetic energy is above or below the potential barrier of the second boundary.

The combined effect of a segment with modified dispersion and linear coefficients is shown in Fig. 5. Curves 2 and 3 show anomalous behavior i.e. a weak repulsive linear potential added to an attractive dispersion potential yields

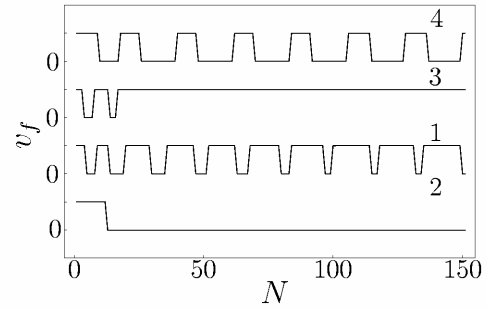


Fig. 5. Capture-transmission patterns for a segment with  $\mu = -0.35$  and different  $\varepsilon$ . Curves 1-4 correspond to  $\varepsilon = 0.0, -0.001, 0.001, 0.005$ , respectively.  $v_0 = 0.05$ .

capture for  $N > 20$  (curve 2), while a weak attractive linear potential yields transmission (curve 3). The explanation is associated with the complex potential profile at the boundary. A dispersion-defect segment has a step in the middle which seems to increase the perturbation at the boundary (Fig. 6, curve 1). Repulsive linear potentials increase the perturbation (curve 2), leading to capture of the soliton, although the combined potential well has become shallower. Attractive linear potentials reduce the perturbation and lead to transmission although the resulting well has become deeper (curve 3). The profile in curve 4 is dominated by the attractive linear potential, which yields the periodic pattern in Fig. 5, curve 4.

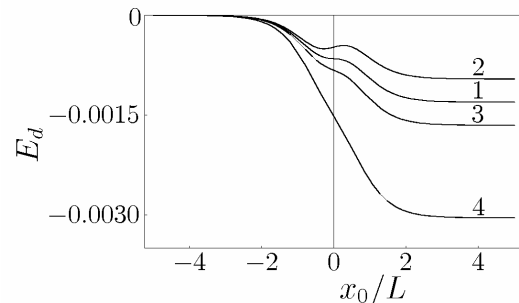


Fig. 6. Potential profiles near the boundary for defect segments with modified dispersion and linear coefficients.  $x_0$  is the distance from the center of the soliton to the boundary. Curves 1-4 correspond to curves 1-4 in Fig. 5.

#### 4. Conclusions

We have studied numerically the interaction of slow solitons with extended defects modeled by inhomogeneous linear, nonlinear and dispersion terms in the NLS equation. In the case of attractive potentials and for a given range of parameters, we have obtained periodically repeating regions of trapping, transmission and reflection as a function of the width of the potential. The effects are explained by an excitation and a following resonant de-excitation of shape oscillations of the solitons at the boundaries of the well, as the period of the capture-

transmission patterns coincides with the period of the shape oscillations. In the non-resonant case, due to loss of kinetic energy, the solitons are trapped inside the well. Whenever the time for which the solitons cross the well is commensurate with the period of the shape oscillations, a resonant inelastic interaction with the second boundary extinguishes the shape oscillations, transferring their energy back into kinetic energy of the solitons and allowing them to escape.

### Acknowledgements

This work is supported in part by the National Science Foundation of Bulgaria under Grant No. F1414.

### References

- [1] M. J. Ablowitz, M. D. Kruskal, J. R. Ladik, *SIAM J. Appl. Math.* **36**, 478 (1979).
- [2] D. K. Campbell, J. F. Schonfeld, C. A. Wingate, *Physica* **9D**, 1 (1983).
- [3] M. Peyrard, D. K. Campbell, *Physica* **9D**, 33 (1983).
- [4] Yu. S. Kivshar, Zhang Fei, L. Vázquez, *Phys. Rev. Lett.* **67**, 1177 (1991).
- [5] Zhang Fei, Yu. S. Kivshar, L. Vázquez, *Phys. Rev. A* **45**, 6019 (1992); **46**, 5214 (1992).
- [6] R. Sharf, A. R. Bishop, *Phys. Rev. A* **46**, R2973 (1992).
- [7] J. J.-L. Ting, M. Peyrard, *Phys. Rev. E* **53**, 1011 (1996).
- [8] H. Frauenkron, P. Grassberger, *Phys. Rev. E* **53**, 2823 (1996).
- [9] G. Kälbermann, *Phys. Lett. A* **252**, 37 (1999); *Chaos, Solitons and Fractals* **12**, 625 (2001), **12**, 2381 (2001).
- [10] Y. Nogami, F. M. Toyama, *Phys. Lett. A* **184**, 245 (1994).
- [11] J. Kaup, *Phys. Rev. A* **42**, 5689 (1990).
- [12] Yu. S. Kivshar, D. E. Pelinovski, T. Cretegny, M. Peyrard, *Phys. Rev. Lett.* **80**, 5032 (1998).
- [13] K. T. Stoychev, M. T. Primatarowa, R. S. Kamburova, *Phys. Rev. E* **73**, 066611 (2006).

---

\*Corresponding author: stoychev@issp.bas.bg